*J. Chem. Sci.* (2020)132:131
https://doi.org/10.1007/s12039-020-01840-y


REGULAR ARTICLE

# Characterization, microbial and catalytic application of $V_2O_5$ nanoparticles prepared from Schiff base complexes as precursor

MOHAMMAD NASIR UDDIN[a,*], MD. SAIFUR RAHMAN[a], WAHHIDA SHUMI[b], MD. KAMRUL HOSSAIN[a] and A K M ATIQUE ULLAH[c]

[a]Department of Chemistry, University of Chittagong, Chittagong 4331, Bangladesh
[b]Department of Microbiology, University of Chittagong, Chittagong 4331, Bangladesh
[c]Nanoscience and Technology Research Laboratory, Chemistry Division, Atomic Energy Center, Bangladesh Atomic Energy Commission, Dhaka 1000, Bangladesh
E-mail: mnuchem@cu.ac.bd; nasircu72@gmail.com

MS received 8 June 2020; revised 4 August 2020; accepted 5 August 2020

**Abstract.** Vanadium pentoxide ($V_2O_5$) nanoparticles have gained much attention due to their simple synthesis, a wide range of chemical, industrial, biological, and medicinal applications including anti-inflammation, anti-oxidant, anti-microbial activities. Vanadium complexes of Schiff bases were used as a precursor to synthesis vanadium pentoxide ($V_2O_5$) nanoparticles. The precursor Schiff base complexes were obtained by mixing vanadyl acetylacetonate with the prepared Schiff base ligands maintaining a ratio 1:1. After that $V_2O_5$ nanoparticles (denoted by C-1, C-2, C-3 and C-4) were synthesized by the direct calcination method based on thermal evaporation-condensation of vanadium complexes at 600 °C for 3 h. Finally, the analytical tools such as FTIR, XRD, EDS and SEM provided evidence in favor of the formation of $V_2O_5$ nanoparticles. In addition, microbial study and photocatalytic activity were carried out using a spectrophotometer. An antimicrobial study showed that all the prepared $V_2O_5$ nanoparticles have inhibition capacity against the growth of some selected human pathogenic bacteria and few of them against plant pathogenic fungi. Moreover, these $V_2O_5$ nanoparticles have photocatalytic activity since these particles degrade organic dye, Eosin yellow.

**Keywords.** Vanadium pentoxide; nanoparticles; microbial; photocatalytic; Eosin yellow.

**Abbreviations**

| | |
|---|---|
| NPs | Nanoparticles |
| HOMO | Highest occupied molecular orbital |
| LUMO | Lowest unoccupied molecular orbital |
| FT-IR | Furrier transfer infrared |
| XRD | X-ray diffraction |
| SEM | Scanning electron microscope |
| EDS | Energy dispersive spectroscopy |
| DMSO | Dimethyl sulfoxide |

## 1. Introduction

Nanostructured one-dimensional (1D) transition metal oxides show greater interest because of their fascinating magnetic, optical, electrical properties in addition to their chemical and thermal stability.[1] Nano-sized Vanadium pentoxide ($V_2O_5$) have gained significant attention due to their structural, chemical and physical properties[2] increasing the surface to volume ratio.[3] It is n-type semiconducting material and the most stable oxide with a wide bandgap ($E_g$) of 2.2-2.3 eV,[4, 5] interesting photocatalysis[6] and electrochemical[7, 8] performances. $V_2O_5$ is used as a catalyst during decarbonylative halogenation of aldehyde.[9, 10] Among $V_2O_5$ nanoparticles, non-bonded d-orbitals of V ions act as Lewis acid and LUMO character, whereas oxygen atoms holding HOMO character, lone pair of electron act as Lewis base.[11] $V_2O_5$ nanoparticles show a better magnetic property, microbial activity (anti-bacterial as well as anti-fungal) and photocatalytic activity.[9, 10] Near 257 °C, $V_2O_5$ undergoes its transition phase and a change in oxide crystal structure at the same time that alters

*For correspondence

*Electronic supplementary material: The online version of this article (https://doi.org/10.1007/s12039-020-01840-y) contains supplementary material, which is available to authorized users.*

Published online: 25 September 2020

electrical and optical behavior.[12] It is known that different nanomaterials show various properties depend on their size and shape.

A variety of physical and chemical methods like ball milling,[13] Sol-gel methods,[14] laser ablation, electrophoretic deposition, chemical vapor deposition,[15] electrochemical depositions, thermal evaporation-condensation method[3] or direct calcination method, solution combustion method and hydrothermal method have been adopted for the preparation of metal oxide nanoparticles.[3, 12, 16–18] However, among all these synthetic methods we used the easiest, cost-effective and least time consuming direct calcination method based on thermal evaporation-condensation that can help to easily prepare different morphologies of nanomaterial.

Herein, the synthesis, characterization and applications of orthorhombic $V_2O_5$ nanoparticles obtained from four different Schiff base complexes are reported and their properties, microbial and photocatalytic behaviors are compared to identify the better one which shows greater activity than others.

## 2. Experimental

### 2.1 *Materials and methods*

A number of materials were used in this experiment. Vanadyl acetylacetonate was purchased from Merck-Schuchardi. Dimethylsulfoxide (DMSO), diethylformamide (DMF) and acetone were purchased from Aldrich Chemical Co. Ltd. Nitric acid, absolute ethanol and chloroform were purchased from Merck. All other chemicals and solvents were used as received, without further purifications and of analytical grade.

### 2.2 *Synthesis of vanadium pentoxide nanoparticles*

The four different complexes have been employed for the preparation of $V_2O_5$ nanoparticles as a precursor. Synthesis of $V_2O_5$ nanoparticles was carried out through an easier direct calcination method. The four vanadium complexes of Schiff bases synthesized by standard procedure[19] were loaded into a silicon crucible individually and placed into a muffle furnace and heated at a rate of 10 °C/min. Nanoparticles of $V_2O_5$ were obtained at 600 °C after 3 h of heating (Figure 1). Then these were allowed to cool. After that they were collected from the crucible and the final products were washed with ethanol for at least 3 times to remove impurities and then dried at room temperature and preserved with vacuum tube.

### 2.3 *Simple characterization*

The four as-synthesized nanoparticles were characterized using magnetometer, FT-IR, XRD, SEM and EDS. The magnetic property was measured in order to confirm the formation of $V^{5+}$. Furrier Transform Infrared (FT-IR) was performed to identify the possible significant functional groups and characteristic peaks of V-O bonding by using Prestige-21, FTIR, SHIMADZU. X-ray diffraction (XRD) studies were carried out using XRD instrument, Philis PANalytical X'PERT-PRO with Cu-Kα radiation to investigate the crystalline phase and also to study the structural integrity of $V_2O_5$. SEM imaging was performed using Scanning Electron Microscope (model, JEOL JSM 7600F, Japan) and EDS studies were carried out through Energy-dispersive X-ray spectroscopy (model, JEOL JSM 7600F, Japan) to determine which chemical elements are present in a sample, and also used to estimate their relative abundance.

### 2.4 *Antimicrobial activities*

The synthesized $V_2O_5$ nanoparticles were tested *in vitro* using liquid media method[20] against two human pathogenic bacteria *Salmonilla typhi* and *Staphylococcus aureus* and three phyto-pathogenic fungi *Aspergillus flavus, Penicillium spp* and *Fusarium spp*. All strains were cultured and collected from Department of Microbiology, University of Chittagong. Strains' identification was confirmed clearly before the test.

2.4a *Antibacterial activities*: Liquid media method[20] was used to investigate the antibacterial activities, measuring absorption through a spectrophotometer at a wavelength of 625 nm. Nutrient agar (NA) and nutrient broth (NB) medium were conducted for the culture of bacteria and DMSO was used as a solvent for the preparation of sample solution.[21] The composition of NB medium as follows: peptone (5 g), beef extract (3 g), NaCl (0.5 g) and distilled water (1000 mL). 5 g peptone, 3 g beef extract and 0.5 g NaCl were added carefully in a 1000 mL distilled water of beaker and mixed thoroughly with a glass rod. The mixed solution was heated to boil about 15 min. After 15 min boiling, the mixture was cooled and then transferred to the test tubes at a volume of 10 mL per test tube. Furthermore, the media containing the test tube was closed with a cotton plug and autoclaved with a test tube holder at 121 °C and 15 psi pressure for 45 min. Then the culturing of microorganisms was performed.

2.4b *Antifungal activity*: Potato Dextrose Agar (PDA) medium was used throughout the study for the growth and maintenance of fungal isolates. Potato Dextrose broth (PDB) medium was used for the antifungal activity observation against the test compounds. PDB solution was prepared by dissolving 200 g potato and 20 g dextrose in 1000 mL of distilled water. The mixture was then boiled for

15 min and autoclaved for 45 min. The PDB medium (50 mL) was dispensed into 200 mL conical flasks. Conical flasks containing 50 mL medium were labelled separately and 100 µL of test compounds (0.1% concentration) were added in each separate conical flask.[22] The flasks were shaken well to mix thoroughly and then 1 mL of fungal suspension was added carefully at each of conical flasks. All the conical flasks were incubated at 27 ± 2 °C for 7 days. A control conical flask was prepared with DMSO solvent to observe the result. After 7 days incubation, the growth of the fungal biomass, spore formation, $p^H$ and color change were checked, observed and recorded.[23]

### 2.5 *Photocatalytic activity*

The photocatalytic activity of $V_2O_5$ nanoparticle (C-2 only) was evaluated using Eosin Yellow (EY) as dye at room temperature. The test was carried out under a 25 W metal halide lamp that emitting 254 nm. The maximum absorbance of EY solution was found at 517 nm. Using this $\lambda_{max}$, the calibration curve was constructed. Testing solutions were prepared by adding 0.3 g $V_2O_5$ and 5 mL EY solution ($10^{-5}$M) in 100 mL distilled water, mixing properly. The solution was kept under UV light with stirring by a magnet in a degradation chamber. About 6 mL of solution was transferred into test tubes 30 min intervals each time for centrifuge and then took absorbance with a transparent solution at 517 nm by spectrophotometer. By knowing the absorbance, percentage of degradation (EY) was calculated using $(A_0 - A)$ 100% $/A_0$ formula, where $A_0$ and A are initial and final absorbance, respectively.

## 3. Results and Discussion

### 3.1 *Structural characterization of $V_2O_5$ nanoparticles*

3.1a *Magnetic property analysis*: Magnetic properties of $V_2O_5$ NPs were carried out using magnetometer at room temperature. The behavior of a compound in a magnetic field is either being diamagnetic, paramagnetic or ferromagnetic.[25] Vanadium contains three electrons in its 3d-orbital and can form three common oxidation states like V(III), V(IV) and V(V). In V(V), no unpaired electron exists in 3d orbital. As a result, it did not show paramagnetic behavior and was rather diamagnetic. $V_2O_5$ nanoparticles showed diamagnetic character which is not attracted by the applied magnetic field. It was confirmed through magnetic susceptibility calculation of prepared $V_2O_5$. Magnetic susceptibility of $V_2O_5$ was found a negative value that confirmed the diamagnetic character of the synthesized compounds as the negative value of magnetic susceptibility indicates diamagnetic nature. The diamagnetic property of the synthesized compounds demonstrated that no unpaired electron was present in the 3d orbital of V which resulted in the formation of $V^{5+}$.[24] As a result, electronic configuration and magnetic susceptibility calculation support the existence of $V^{5+}$.

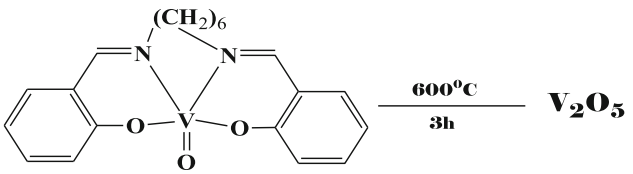


**Figure 1.** $V_2O_5$ nanoparticles prepared from VO(Sal-Hn-Sal) complex.

3.1b *FT-IR analysis*: FT-IR measurement was performed to identify the possible significant functional groups and the characteristics peak of V-O bonding. IR spectra of C-1, C-2, C-3 and C-4 nanoparticles are shown in Figure S1 (Supplementary Information). In the following figures, there was no broad peak at 3200 to 3500 $cm^{-1}$ due to the absence of O-H stretch (H-bonded alcohols). But nanoparticles are capable in absorbing moisture from surrounding by having a high surface area to volume ratio.[26] In the infrared spectra of the prepared nanoparticles, the broad peak observed in the region of 477–600 $cm^{-1}$ is the characteristic peak of V-O bonding. Similarly, the broad peak at 823–829 $cm^{-1}$ was observed due to the presence to V-O-V bonding.[27] The broad peak at 1017–1022 $cm^{-1}$ was observed due to the presence to V=O bonding.[28] The peaks at 470 $cm^{-1}$, 492 $cm^{-1}$, 829 $cm^{-1}$ and 1018 $cm^{-1}$ indicated the formation of the $V_2O_5$ nanoparticles and also support the presence of orthorhombic phase. [29]

3.1c *XRD analysis*: The crystal phase and crystallinity of as-synthesized $V_2O_5$ nanoparticles were investigated by XRD. Figure 2 shows that the $V_2O_5$ nanoparticles are in the crystalline form of an orthorhombic system. XRD peaks confirm that the formation of $V_2O_5$ from each precursor was in orthorhombic phase compared to standard $V_2O_5$ (JCPDS NO 89-2483) with calculated lattice constants a = 3.563 Å, b = 11.510 Å, c = 4.369 Å.

The main characteristic diffraction peaks are observed at $2\theta$ values (20.448°, 26.336°, 31.196°, 32.517°, 34.479°, 41.41°, 47.477° and 51.331°) and corresponding orthorhombic phase of $V_2O_5$ crystal planes (001), (110), (301), (011), (310), (310), (600)

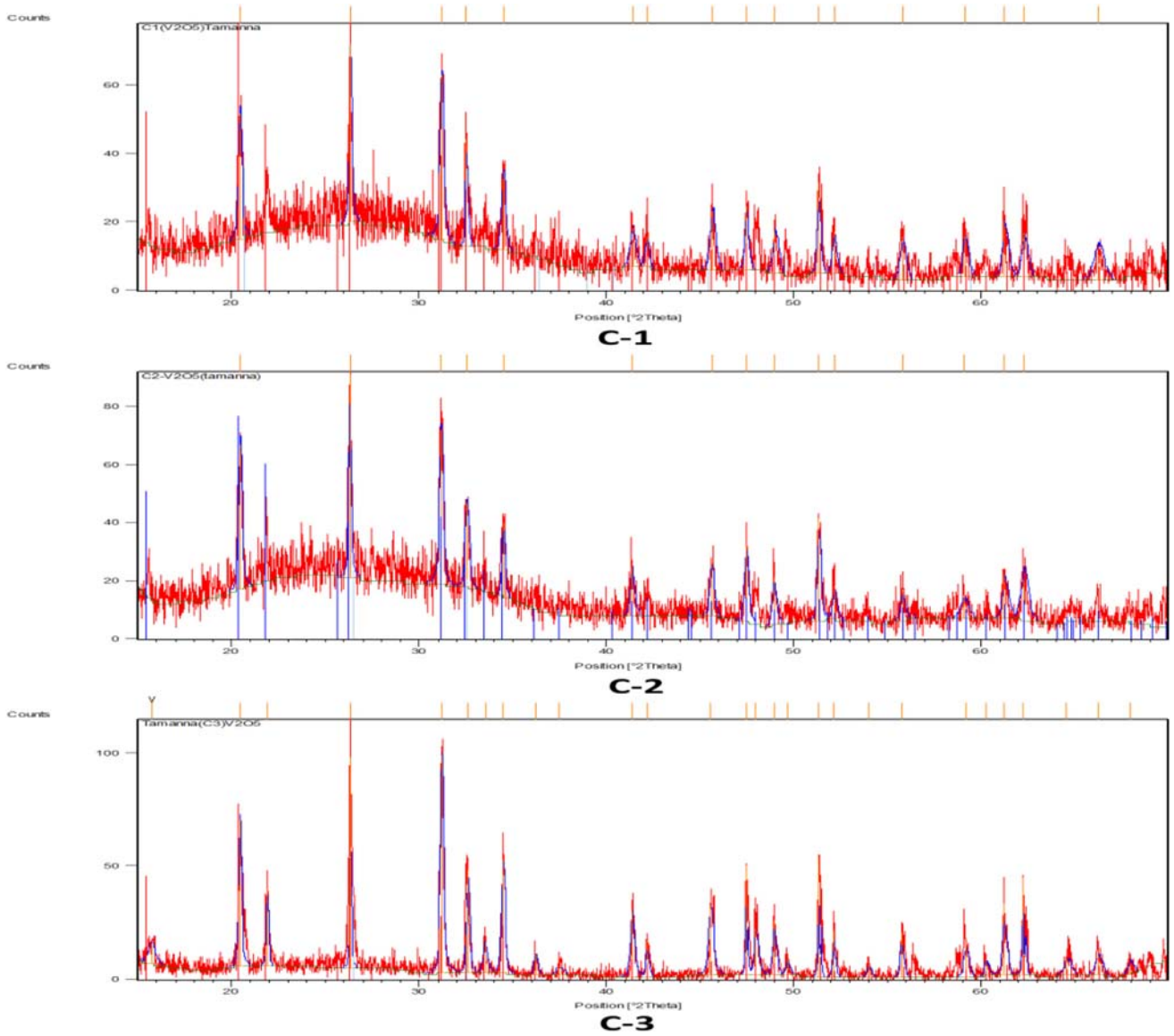


**Figure 2.** X-ray diffraction patterns of $V_2O_5$ nanoparticles (C-1, C-2 and C-3).

and (020), respectively. There was no other significant peak detected, indicating the purity of $V_2O_5$ products.[30] The average particle size utilizing Debye-Scherrer formula, $D = 0.9\lambda/\beta \cos\theta$; where D is average particle size, $\lambda$ is the X-ray wavelength (0.1541 nm), $\beta$ and $\theta$ are the full widths at half-maximum (FWHM) and the diffraction angles respectively, was ascertained 36.60 nm (C-1), 36.93 nm (C-2), 42.90 nm (C-3) and 15.63 nm (C-4).

3.1d *SEM analysis*: The SEM images of as-prepared $V_2O_5$ nanoparticles focused on the surface morphologies and structural information. The SEM images of C-3 and C-4 obtained from the different precursor are shown in Figure 3. With the decrease of the size of particles, increases the surface area that increases the capacity as well.[31–33] Figure 3 shows the prepared particles through thermal evaporation-condensation method produce of flake-like structure which is agglomerated. SEM image shows that both C-3 and C-4 $V_2O_5$ nanoparticles are distributed randomly and having good crystalline morphology.

3.1e *EDS analysis*: Energy-dispersive X-ray spectroscopy (EDS) is a very sophisticated and important analytical tool used to elemental analysis, chemical characterization of sample, estimate relative abundance and to identify the percentage of elements present in the materials.[34] EDS demonstrates (Figure 4) the presence of V and O peak only (confirmed by IR also). The corresponding chemical composition of $V_2O_5$ nanoparticles in C-3 and C-4 are

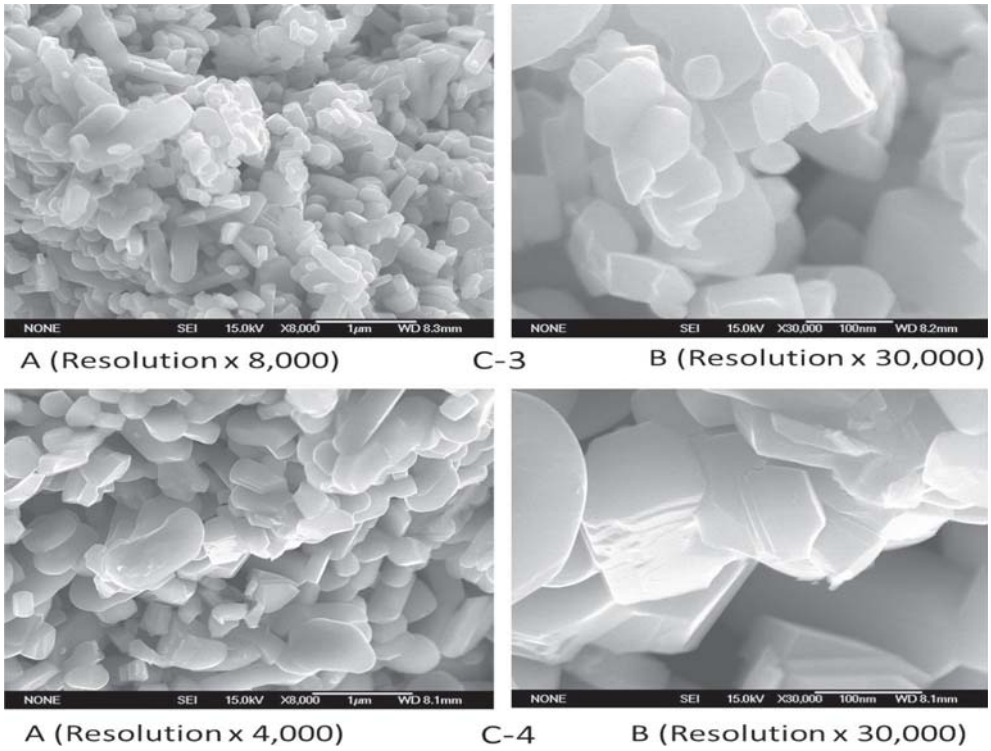


**Figure 3.** SEM images of $V_2O_5$ nanoparticles, C-3 and C-4.

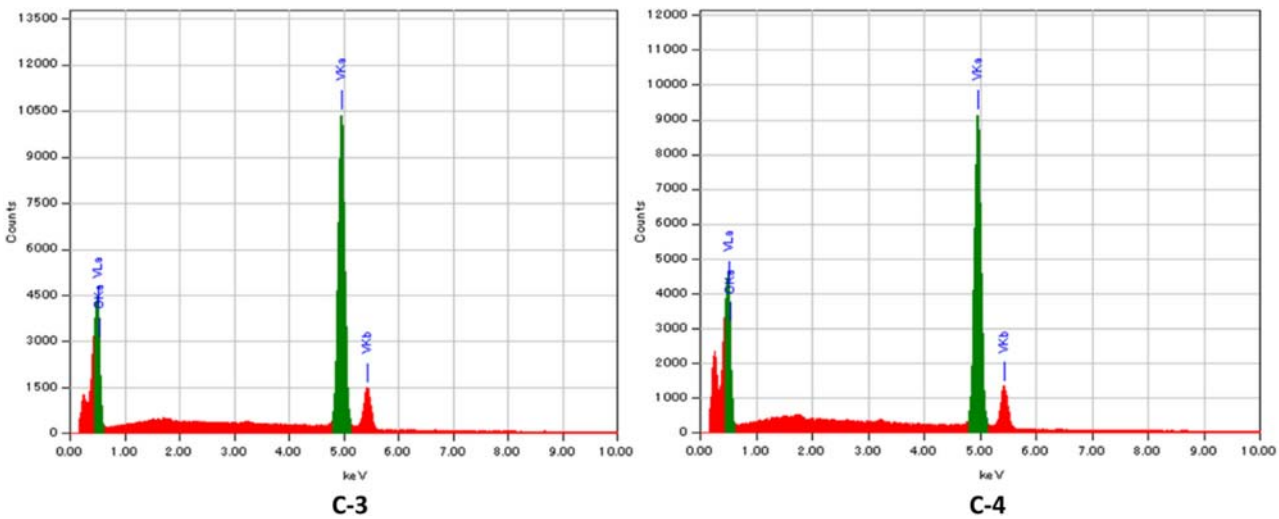


**Figure 4.** EDS image of synthesized $V_2O_5$ nanoparticles, C-3 and C-4.

63.42% and 57.46% of V as well as 36.58% and 42.54% of O, respectively, indicating the purity of the samples.

## 3.2 *Microbial assessments*

3.2a *Antibacterial activity analysis*: The effects of antibacterial activity were studied by liquid culture method.[35] Inhibition of bacterial growth in the presence of $V_2O_5$ nanoparticles from 3 h to 24 h was investigated. The optical densities were recorded at one concentration (0.10%) only for all bacteria. Figure 5 depicts the percentage of growth inhibition for human pathogenic bacteria *S. typhi*, showing inhibition capacity of organism growth during the incubation period. C-1 at 12 and 21 h, C-2 at 18 and 24 h, C-3 at 18 h, C-4 at 18 and 21 h showing very much effective against *S. typhi*. Results (Figure S2, Supplementary Information) of growth inhibition for

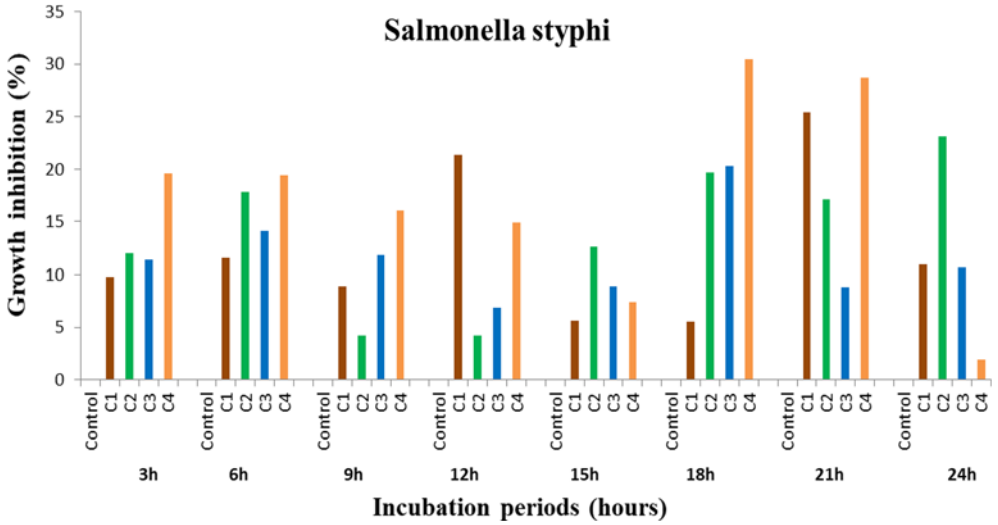


**Figure 5.** Growth inhibition of *Salmonella typhi* with $V_2O_5$ nanoparticles, C-1, C-2, C-3 and C-4.

**Table 1.** Change of $p^H$ for test organisms after 7 day incubation at 27 °C.

| | | *Aspergillus flavus* | | *Penicillium* spp. | | *Fusarium* spp. | |
|---|---|---|---|---|---|---|---|
| Symbol | Initial | Final | Test | Final | Test | Final | Test |
| Control | 6.0 | 5.6 | 4.4 | 5.6 | 4.5 | 5.6 | 4.4 |
| C-1 | 6.5 | 4.7 | 4.2 | 4.7 | 4.1 | 4.7 | 4.2 |
| C-2 | 6.2 | 5.5 | 4.3 | 5.5 | 4.2 | 5.5 | 4.3 |
| C-3 | 5.3 | 4.9 | 1.6 | 4.9 | 4.0 | 4.9 | 1.6 |
| C-4 | 6.0 | 4.9 | 4.2 | 4.9 | 4.2 | 4.9 | 4.2 |

human pathogenic bacteria *S. aureus* showed inhibition capacity of organism growth during the incubation period. Against bacteria *S. aureus*, all nanoparticles were supporting greater effectiveness as the incubation period increased. In both cases, the growth of control (without sample) was considered 100% (no inhibition). It is clear that the prepared nanoparticles are showing inhibiting activity, not inducing activity against the test organisms, i.e., antibacterial properties exist.

3.2b *Antifungal activity analysis*: Antifungal activities of synthesized nanoparticles were assessed by liquid media method. The result was recorded through $p^H$ measurement of the solutions and weighing dry biomass against *Aspergillus flavus, Penicillium spp* and *Fusarium spp.* By collecting the experimental data, it is clear that C-1, C-2 and C-3 are showing the inducing capacity for *Aspergillus flavus* (C-3 also for *Fusarium spp.*) but C-4 showing greater inhibition capacity due to small size, indicating antifungal properties. Change of $p^H$ and color change due to spore formation are tabulated in Tables 1 and 2, respectively. Figure 6 shows the weight of biomass collected from antifungal experiments of synthesized nanoparticles against the test organisms.

### 3.3 *Photocatalytic activity analysis*

The photocatalytic experiment was conducted in the atmospheric system. The experimental results are presented in Figure 7. The experimental data were collected in two ways to confirm the photocatalytic activities such as catalytic and photolytic. Photolytic degradation of EY was done in the absence of metal oxide nanoparticles. From Figure 7, the absorbance of the solution was found to be almost same, indicating zero degradation. Catalytic degradation was carried out using $V_2O_5$ nanoparticles not only in the absence of light but also in the presence of UV light to compare the result. It is seen that only 4.33% degradation

**Table 2.** Change of color for test organisms after 7 day incubation at 27 °C.

| Symbol | Initial | *Aspergillus flavus* Final | *Penicillium* spp. Final | *Fusarium* spp. Final |
|---|---|---|---|---|
| Control | Fade | Black-huge white mat, Black spore | White-only mat | White mat, no spore |
| C-1 | Fade | Fade-no mat, formation occur | Premature spores | No mat |
| C-2 | Fade | Light brown-only mat | No mat, only spore | No mat |
| C-3 | Fade | White-Scanty mat | Light brown-only spore | While mat with brownish spore |
| C-4 | Fade | Light brown-White mat with brownish sporulation | No spore, only huge mats | Only mat |

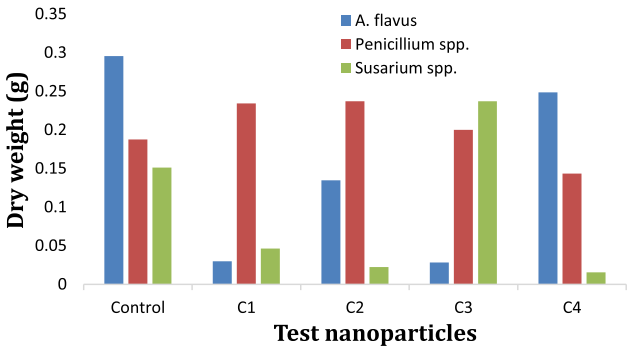


**Figure 6.** Weight of biomass measurement after 7 day incubation at 27 °C.

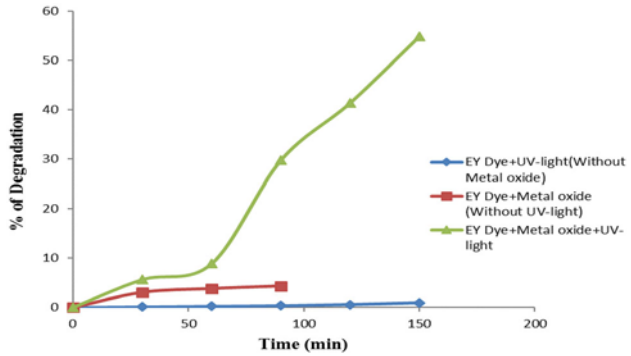


**Figure 7.** Photocatalytic degradation (%) of EY dye with time.

in the absence of UV-light occurred. However, in the presence of UV-light, the considerable amount of dye was degraded by $V_2O_5$ nanoparticles and 54.89% degradation was observed. It is clear that there are least differences between the first two FTIR spectra (Figure S3 a, b, Supplementary Information) taken without UV-light. It is caused due to the only adsorption of EY dye on $V_2O_5$ nanoparticles. But quite a different spectrum of EY dye was obtained when a similar experiment was done in the presence of UV-light (Figure S3 c, Supplementary Information). It is because there are many functional groups and bonds that have been destroyed and new bonds and functional groups have been created. These results conclude that $V_2O_5$ nanoparticles can be a good catalyst against EY.

## 4. Conclusions

$V_2O_5$ nanoparticles were synthesized by direct calcination method based on thermal evaporation-condensation. The properties of as-synthesized $V_2O_5$ nanoparticles are studied by FT-IR, XRD, SEM and

EDS. $V_2O_5$ nanoparticles were found in diamagnetic nature. The XRD pattern indicated that all $V_2O_5$ nanoparticles were orthorhombic phase with the average crystalline size of 36.60 nm (C-1), 36.93 nm (C-2), 42.90 nm (C-3) and 15.63 nm (C-4). The FT-IR confirmed the formation of $V_2O_5$ nanoparticles. SEM images focused on surface area and crystal morphology. EDS study supports the purity and relative abundance of the nanoparticles. From the antimicrobial study, it is identified that C-4 nanoparticle has greater inhibition capacity because of its small size than others against the growth of human pathogenic bacteria *S. typhi* and *S. aureus* as well as plant pathogenic fungi *Aspergillus flavus, Penicillium spp.* and *Fusarium spp*. Finally, good photocatalytic degradation of Eosin yellow was found for synthesized $V_2O_5$ nanoparticles.

## Supplementary Information (SI)

Figures S1-S3 are available at www.ias.ac.in/chemsci.

## Acknowledgements

The authors acknowledge Md. Moniruzzaman of Shizuoka University, Japan for the timely help in characterization studies.

## ReferenceS

1. Al Zoubi M, Farag H K and Endres F 2009 Sol–gel synthesis of vanadium pentoxide nanoparticles in air- and water-stable ionic liquids *J. Mater. Sci.* **44** 1363
2. Zhou F, Zhao X, Yuan C and Li L 2008 Vanadium pentoxide nanowires: hydrothermal synthesis, formation mechanism, and phase control parameters *Cryst. Growth Des.* **8** 723
3. Raj A T, Ramanujan K, Thangavel S, Gopalakrishan S, Raghavan N and Venugopal G 2015 Facile synthesis of vanadium-pentoxide nanoparticles and study on their electrochemical, photocatalytic properties *J. Nanosci. Nanotechnol.* **15** 3802
4. Cogan S F, Nguyen N M, Perrotti S J and Rauh R D 1989 Optical properties of electrochromic vanadium pentoxide *J. Appl. Phys.* **66** 1333
5. Chain E E 1991 Optical properties of vanadium dioxide and vanadium pentoxide thin films *Appl. Opt.* **30** 2782
6. Nair D P, Sakthivel T, Nivea R, Eshow J S and Gunasekaran V 2015 Effect of surfactants on electrochemical properties of vanadium-pentoxide nanoparticles synthesized *via* hydrothermal method *J. Nanosci. Nanotechnol.* **15** 4392
7. Pereira-Ramos J P, Messina R and Perichon J 1986 Electrochemical behaviour of some transition metal oxides in molten dimethylsulphone at 150°C *J. Appl. Electrochem.* **16** 379
8. Park H, Smyrl W H and Ward M D 1995 $V_2$ $O_5$ xerogel films as intercalation hosts for lithium: I. insertion stoichiometry, site concentration, and specific energy *J. Electrochem. Soc.* **142** 1068
9. Rana S, Pandey B, Dey A, Haque R, Rajaraman G and Maiti D 2016 A doubly biomimetic synthetic transformation: catalytic decarbonylation and halogenation at room temperature by vanadium pentoxide *Chem. Cat. Chem.* **8** 3367
10. Rana S, Haque R, Santosh G and Maiti D 2013 Decarbonylative halogenation by a vanadium complex *Inorg. Chem.* **52** 2927
11. Haber J, Witko M and Tokarz R 1997 Vanadium pentoxide I. Structures and properties *Appl. Catal. A Gen.* **15 7**3
12. Dai H, Wong E W, Lu Y Z, Fan S and Lieber C M 1995 Synthesis and characterization of carbide nanorods *Nature* **375** 769
13. Subba Reddy C V, Park K-I, Mho S, Yeo I-H and Park S-M 2008 Simple preparation of $V_2o_5$ nanostructures and their characterization *Bull. Korean Chem. Soc.* **29** 2061
14. Cheng K-C, Chen F-R and Kai J-J 2006 $V_2o_5$ nanowires as a functional material for electrochromic device *Sol. Energy Mater. Sol. Cells* **90** 1156
15. Chan C K, Peng H, Twesten R D, Jarausch K, Zhang X F and Cui Y 2007 Fast, completely reversible Li insertion in vanadium pentoxide Nanoribbons *Nano Lett.* **7** 490
16. Nag J and Haglund R F J 2008 Synthesis of vanadium dioxide thin films and nanoparticles *J. Phys. Condens. Matter* **20** 264016
17. Kaid M A 2006 Characterization of electrochromic vanadium pentoxide thin films prepared by spray pyrolysis *Egypt. J. Solids* **29** 273
18. Takahashi K, Limmer S J, Wang Y and Cao G 2004 Synthesis and electrochemical properties of single-crystal $V_2o_5$ nanorod arrays by template-based electrode position *J. Phys. Chem. B* **108** 9795
19. Ajlouni AM, Taha Z A, Al Momani W, Hijazi A K and Ebqäai M 2012 Synthesis, characterization, biological activities, and luminescent properties of lanthanide complexes with *N,N′*-bis(2-hydroxy-1-naphthylidene)-1,6-hexadiimine *Inorg. Chim. Acta* **388** 120
20. Krings U and Berger R G 2001 Antioxidant activity of some roasted foods *Food Chem.* **72** 223
21. Uddin M N, Khandaker S, Amin M S, Shumi W, Rahman M A and Rahman S M 2018 Synthesis, characterization, molecular modeling, antioxidant and microbial properties of some titanium(IV) complexes of Schiff bases *J. Mol. Struct.* **1166** 79
22. Ishikawa N K, Kasuya M C M and Vanetti M C D 2001 Antibacterial activity of lentinula edodes grown in liquid medium *Braz. J. Microbiol.* **32** 206
23. UmaV, Kanthimathi M, Subramanian J and Nair B U 2006 A new dinuclear biphenylene bridged copper(II) complex: DNA cleavage under hydrolytic conditions *Biochim. Biophys. Acta (BBA)-Gen. Subj.* **1760** 814
24. Carlin R L and van Duyneveldt A J 1977 *Magnetic properties of transition metal compounds* (Berlin Heidelberg: Springer-Verlag)

25. Uddin M N, Siddique Z A, Mase N, Uzzaman M and Shumi W 2019 Oxotitanium(IV) complexes of some bis-unsymmetric Schiff bases: synthesis, structural elucidation and biomedical applications *Appl. Organomet. Chem.* **33** e4876
26. Deki S, Akamatsu K, Yano T, Mizuhata M and Kajinami A 1998 Preparation and characterization of copper(I) oxide nanoparticles dispersed in a polymer matrix *J. Mater. Chem.* **8** 1865
27. Menezes W G, Reis D M, Benedetti T M, Oliveira M M, Soares J F, Torresi R M and Zarbin A J G 2009 $V_2O_5$ Nanoparticles obtained from a synthetic bariandite-like vanadium oxide: Synthesis, characterization and electrochemical behavior in an ionic liquid *J. Colloid Interface Sci.* **337** 586
28. Sediri F, Touati F and Gharbi N 2007 A one-step hydrothermal way for the synthesis of vanadium oxide nanotubes containing the phenylpropylamine as template obtained via non-alkoxide route *Mater. Lett.* **61** 1946
29. Levi R, Bar-Sadan M, Albu-Yaron A, Popovitz-Biro R, Houben L, Shahar C, Enyashin A, Seifert G, Prior Y and Tenne R 2010 Hollow $V_2O_5$ Nanoparticles (fullerene-like analogues) prepared by laser ablation *J. Am. Chem. Soc.* **132** 11214
30. Shi S, Cao M, He X and Xie H 2007 Surfactant-assisted hydrothermal growth of single-crystalline ultrahigh-aspect-ratio vanadium oxide nanobelts *Cryst. Growth Des.* **7** 1893
31. Oyama S T, Middlebrook A M and Somorjai G A 1990 Kinetics of ethane oxidation on vanadium oxide *J. Phys. Chem.* **94** 5029
32. Lopez R, Boatner L A, Haynes T E, Feldman L C and Haglund R F 2002 Synthesis and characterization of size-controlled vanadium dioxide nanocrystals in a fused silica matrix *J. Appl. Phys.* **92** 4031
33. Bell R C, Zemski K A, Kerns K P, Deng H T and Castleman A W 1998 Reactivities and collision-induced dissociation of vanadium oxide cluster cations *J. Phys. Chem. A* **102** 1733
34. Matassoni L, Pratesi G, Centioli D, Cadoni F, Lucarelli F, Nava S and Malesani P 2011 Saharan dust contribution to $Pm_{10}$, $Pm_{2.5}$ and $Pm_1$ in urban and suburban areas of Rome: A comparison between single-particle Sem-Eds analysis and whole-sample pixe analysis *J. Environ. Monit.* **13** 732
35. Kenters N, Henderson G, Jeyanathan J, Kittelmann S and Janssen P H 2011 Isolation of previously uncultured rumen bacteria by dilution to extinction using a new liquid culture medium *J. Microbiol. Methods* **84** 52